

Low-Resistance Ti/Al Ohmic Contact on Undoped ZnO

SOO YOUNG KIM,¹ HO WON JANG,¹ JONG KYU KIM,¹
CHANG MIN JEON,¹ WON IL PARK,¹ GYU-CHUL YI,¹
and JONG-LAM LEE^{1,2}

1.—Department of Materials Science and Engineering, Pohang University of Science and Technology (POSTECH), Pohang, Kyungbuk 790-784, Korea. 2.—E-mail: jllee@postech.ac.kr

We report a low-resistance ohmic contact on undoped ZnO using a promising contact scheme of Ti/Al. Specific-contact resistivity, as low as $9.0 \times 10^{-7} \Omega\text{cm}^2$, was obtained from the Ti (300 Å)/Al (3,000 Å) contact annealed at 300°C. It was found that TiO was produced, and the atomic ratio of Zn/O was dramatically increased after annealing at 300°C. This provides the evidence that a number of oxygen vacancies, acting as donors for electrons, were produced below the contact. This leads to the increase of electron concentration via the reduction of contact resistivity.

Key words: ZnO, ohmic contact, photoemission spectroscopy

INTRODUCTION

In recent years, wide-bandgap semiconductor materials, such as ZnO, ZnSe, and GaN, have attracted much attention for the development of blue light-emitting diodes and laser diodes.^{1,2} The properties of ZnO are similar to those of GaN, such as bandgap energy (ZnO: 3.3 eV and GaN: 3.4 eV) and the lattice parameters (ZnO: $a = 0.325$ nm, $c = 0.521$ nm and GaN: $a = 0.319$ nm, $c = 0.519$ nm). Thus, the use of ZnO as a substrate or buffer layer for GaN-based heteroepitaxial growth for overcoming the difficulty in bulk-GaN growth has been reported.³ In particular, ZnO has some notable properties of the large bond strength and the extreme stability of excitons, offering the prospect of practical lasers with low threshold even at high temperature.^{4,5} Especially, undoped-ZnO film is promising as a transparent electrode, not only for its simplicity but also for its high mobility and high transmittance in the long wavelength region compared to doped-ZnO films. To fabricate a high-performance optoelectronic device, low-resistance ohmic contacts are essential. Only a few results for ohmic-contact formation on ZnO were reported.^{6,7} However, detailed studies of ohmic contact on undoped ZnO have not been performed yet. The Gibbs free energy of formation for TiO is much

lower than that for ZnO.⁸ So, the formation of TiO could produce O vacancies (V_O), acting as donors for electrons in ZnO.^{9,10} Furthermore, Ti/Al bilayer metallization is an effective ohmic contact for wide-bandgap semiconductors because of the formation of the intermediate phase of Al_3Ti .¹¹ Therefore, it is expected that a low-resistance ohmic contact could be achieved using Ti/Al metallization on ZnO.

In this paper, we report a Ti/Al ohmic contact to undoped ZnO as a function of annealing temperature. The microstructure at the interface of the contact metal with ZnO was analyzed by x-ray diffraction (XRD). Synchrotron radiation photoemission spectroscopy (SRPES) was employed to examine the change of atomic composition at the interface of Ti with ZnO as a function of annealing temperature. From this, the ohmic-contact formation mechanism on a Ti/Al contact on ZnO is discussed.

EXPERIMENTAL PROCEDURE

The ZnO films used in this work were grown by metal-organic chemical-vapor deposition on a (0001) sapphire substrate. An undoped-ZnO layer with a thickness of 0.2 μm was grown. The electron concentration was $1.7 \times 10^{18} \text{ cm}^{-3}$, and the electron mobility was $59.7 \text{ cm}^2/\text{Vs}$, determined by Hall measurements. The sample was degreased, using acetone and isopropan alcohol with ultrasonication, and rinsed in deionized water. The ZnO samples were

(Received November 19, 2001; accepted May 7, 2002)

etched using Cl_2 and BCl_3 inductively coupled plasma to form a mesa structure. For measurement of the contact resistivity, linear-transmission line pads with gap spacings ($5\ \mu\text{m}$, $10\ \mu\text{m}$, $20\ \mu\text{m}$, $30\ \mu\text{m}$, $40\ \mu\text{m}$, and $50\ \mu\text{m}$) between the pads were patterned by photoresist. The patterned sample was deposited with Ti ($300\ \text{\AA}$) and Al ($3,000\ \text{\AA}$) metals in sequence by electron-beam evaporator. Current-voltage (I-V) measurements were carried out by the four-point probe technique.

To investigate the chemical-bonding states between Ti and ZnO by SRPES, a single layer of Ti ($20\ \text{\AA}$) was deposited using an electron-beam evaporator. The grown sample was cleaned using the same method mentioned previously and loaded into an ultrahigh vacuum chamber (base pressure of $\sim 10^{-10}$ torr), equipped with an electron analyzer and heating element, at the 4B1 beam line in the Pohang Accelerator Laboratory. An incident-photon energy of $600\ \text{eV}$ was used to obtain Zn 3p, O 1s, and Ti 2p core-level spectra. The onset of photoemission, corresponding to the vacuum level at the surface of the Ti-coated ZnO, was measured using an incident-photon energy of $250\ \text{eV}$ with a negative bias on the sample. The incident-photon energy was calibrated with the core-level spectrum of Au 4f.

RESULTS AND DISCUSSION

The specific-contact resistivity of the Ti/Al contact on undoped ZnO is summarized in Table I. To determine the specific-contact resistivity, resistances for the each spacing were measured at a voltage of $0\ \text{V}$. The specific-contact resistivity for the sample annealed at 300°C was evaluated to be $9.0 \times 10^{-7}\ \Omega\text{cm}^2$.

Figure 1 shows XRD profiles of the Ti/Al contact as a function of the annealing temperature. At the as-deposited state, Ti and Al layers were, respectively, deposited along (002) and (001) directions, which are the preferred orientations on a (0001) ZnO. When the sample was annealed at 300°C , a new peak, corresponding to TiO or TiO_2 , was observed. The Gibbs free-energy change per mole of oxygen from thermodynamic data⁸ shows that TiO is a more stable phase than TiO_2 at all temperatures. This means that oxygen atoms in ZnO reacted with the Ti layer to form TiO. After annealing at 500°C , the TiO peak disappeared, but an Al_2O_3 peak appeared.

The chemical composition at the interface of Ti with ZnO was characterized as a function of anneal-

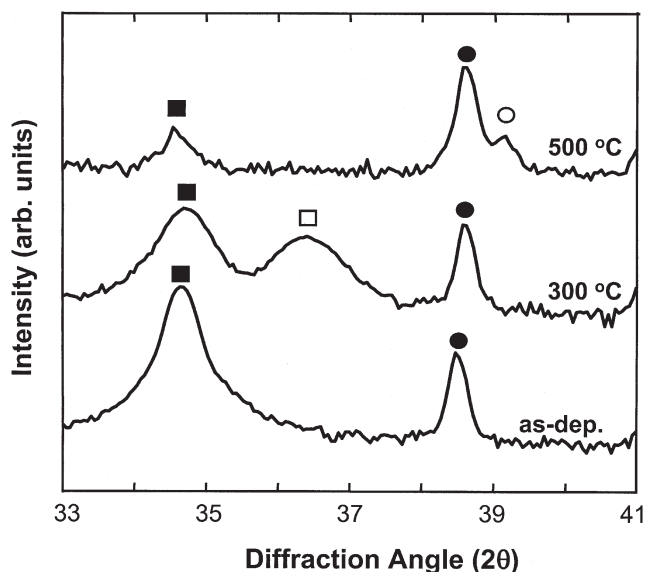


Fig. 1. The XRD profiles as a function of annealing temperature [■: ZnO(002); □: TiO(111); ●: Ti(002) and Al (111); and ○: Al_2O_3].

ing temperature using SRPES. Figure 2a exhibits the x-ray photoelectron spectroscopy (XPS) spectra of O 1s photoelectrons for samples at normal detection. To separate the chemical-bonding states, including in the shoulder, a spectral-synthesis approach was used. The spectral-line shape was simulated using a suitable combination of Gaussian functions. The spectra showed asymmetry at the as-deposited state, but it became symmetric as annealing temperature increased. Thus, two components, one bulk component of O-Zn and one surface component of O-Ti, were considered. In the separation, the full-width-at-half-maximum (FWHM) was fixed with a constant value: $1.9\ \text{eV}$ for the O-Ti bond and $2.3\ \text{eV}$ for the O-Zn bond. The binding energy of the O-Zn bond was higher than that of the O-Ti one, which agrees well with a previously reported value.¹² As annealing temperature increased, the peak intensity corresponding to the O-Ti bond in-

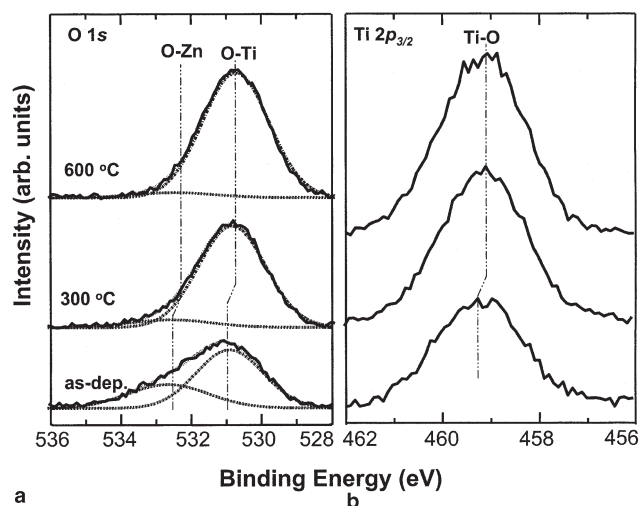


Fig. 2. The XPS spectra of the Ti ($20\ \text{\AA}$)/ZnO sample as a function of annealing temperature: (a) O 1s and (b) Ti 2p.

Table I. Specific-Contact Resistivities in Ti/Al Contacts with Annealing Temperature

Annealing Temperature	Specific-Contact Resistivity (Ωcm^2)
As-deposited	7.3×10^{-6}
200°C	1.2×10^{-6}
300°C	9.0×10^{-7}
400°C	4.5×10^{-6}
500°C	3.6×10^{-4}

creased, meaning the formation of TiO. The peaks of O-Zn and O-Ti shifted about 0.2 eV toward lower binding energy. The XPS spectra of Ti 2p photoelectrons are shown in Fig. 2b. The Ti 2p spectra were symmetric and coincided with the Gaussian fit line, indicating Ti-O bond. No change in the FWHM independent of annealing temperature was observed. The Ti oxides have been already formed even at the as-deposited state. This is due to the fact that Ti reacted with oxygen atoms during air exposure before sample loading to the SRPES chamber. The peaks shifted toward lower binding energy about 0.2 eV. This is consistent with the shift of the O-Zn bond in Fig. 2a. Both results in Fig. 2a and b suggest that Fermi level, E_F , at the surface of ZnO shifts by 0.2 eV to valence-band maximum, that is, the increase in the effective Schottky barrier height (SBH) for electron transport.

The atomic concentrations of each element were calculated from the integration of Zn 3p, Ti 2p, and the O 1s spectra, summarized in Table II. The ratio of $Zn/O_{[O-Zn]}$ with annealing temperature is plotted in Fig. 3. The subscript marked in parenthesis means the type of O bond in ZnO. The value of the $Zn/O_{[O-Zn]}$ ratio on the as-deposited sample was set as 1.0 for reference. After annealing at 300°C, the ratio increased. This means that oxygen atoms were out-diffused from ZnO, resulting in the production of oxygen vacancies, V_O , at the interface region. When the sample was annealed at 500°C, the ratio decreased, meaning the out-diffusion of both Zn and O atoms.

Table II. Atomic Concentration of Each Element Calculated from the Integration of the Zn 3p, Ti 2p, and O 1s Spectra for the Ti (20 Å)/ZnO Sample

Annealing Temperature (°C)	O			
	Zn	Ti	O-Ti	O-Zn
As-deposited	0.34	0.24	0.28	0.14
300°C	0.36	0.25	0.35	0.04
500°C	0.12	0.34	0.51	0.02

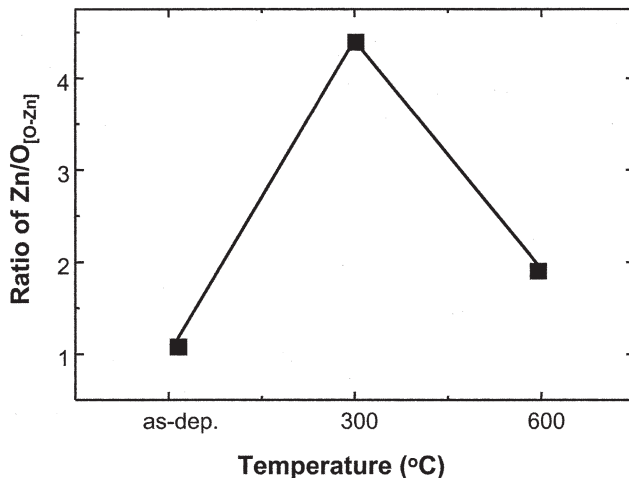


Fig. 3. The change of the $Zn/O_{[O-Zn]}$ atomic ratio with annealing temperature (set as 1.0 for reference for the sample before annealing).

The relative change of work function with the annealing temperature was measured using secondary electron-emission spectra, as shown in Fig. 4. The onset of the secondary-electron peak shifts toward higher kinetic energies with the increase of annealing temperature, indicating that the work function of the contact increased through the annealing. Compared to the as-deposited sample, the work function was increased by 0.4 eV after annealing at 300°C and 0.8 eV after annealing at 600°C. This could be due to the formation of TiO and Al_2O_3 oxides, leading to the increase of the SBH for electron injection from metal layer to ZnO.

The improvement in contact resistivity after annealing at 300°C can be explained with the energy-band diagram below the interface of Ti/ZnO, as shown in Fig. 5. When the sample was annealed at 300°C, the SBH was increased due to the formation of TiO, as shown in Fig. 2. However, a number of V_O were created at the interfacial contact region. Because V_O act as donors in ZnO,^{9,10} degenerated ZnO below the contact can be formed, and thus, electron

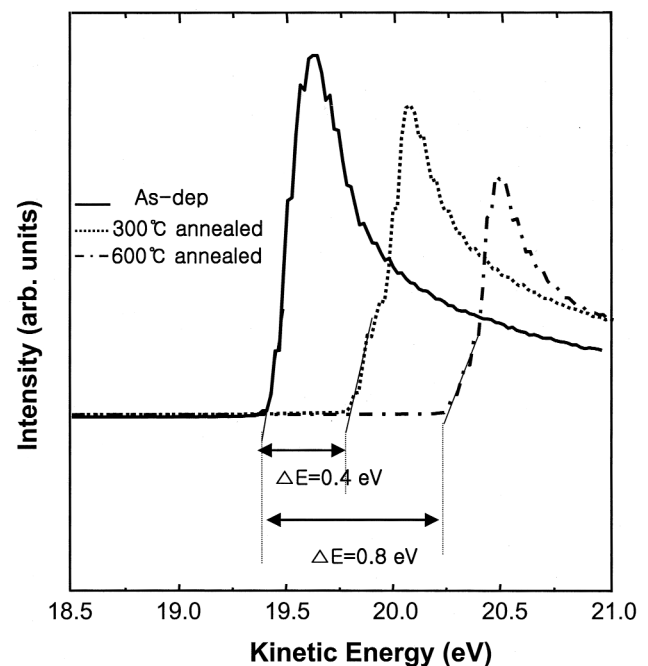


Fig. 4. The secondary electron-emission spectra for the Ti contact on ZnO before and after annealing at 300°C.

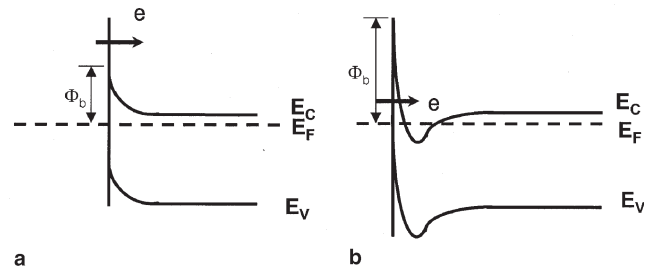


Fig. 5. The schematic energy-band diagram below the interfaces of Ti/ZnO: (a) as-deposited and (b) annealed at 300°C. After annealing, degenerated ZnO was formed below the contact interface.

tunneling by the field-emission mechanism becomes predominant, resulting in a decrease of contact resistivity.

Based on experimental observations in Figs. 1 and 2, the annealing-temperature dependence of specific-contact resistivity could be explained as follows. After annealing at 300°C, XRD and XPS data showed that Ti reacted with oxygen atoms to form TiO, leaving V_O in ZnO. Because the Gibbs free-energy change per mole of oxygen for TiO ($\Delta G_{600} = -967.714$ kJ/mole) is much lower than that for ZnO ($\Delta G_{600} = -580.904$ kJ/mole),⁸ the formation of TiO is preferable after annealing at 300°C. The V_O , acting as donors, are located at shallow levels with an energy about 20–40 meV below the conduction-band edge,⁹ resulting in the production of electrons. Thus, it could be explained that the improvement in electrical property of the annealed Ti/Al contacts is due to the increase in the electron concentration near the surface of ZnO. After annealing at 500°C, XRD data showed that the Al_2O_3 peak appears instead of the TiO peak because the Gibbs free energy per mole of oxygen for Al_2O_3 ($\Delta G_{800} = -949.925$ kJ/mole) is lower than that for TiO ($\Delta G_{800} = -929.756$ kJ/mole).⁸ The Al_2O_3 acts as an insulator, leading to the increase of the specific-contact resistivity.

CONCLUSIONS

A specific-contact resistivity as low as 9.0×10^{-7} Ωcm^2 was achieved on undoped ZnO by annealing the Ti (300 Å)/Al (3,000 Å) contact at 300°C. After annealing at 300°C, increases in Ti-O and O-Ti bonds were found, meaning the formation of TiO. The increase in atomic ratio of $Zn/O_{[O-Zn]}$ supports

that a number of V_O were produced in ZnO. Therefore, the electron concentration near the surface of ZnO increases, leading to the reduction of contact resistivity. After annealing at 500°C, Al_2O_3 phase was formed, which could lead to the degradation of the device with this contact metallization.

ACKNOWLEDGEMENT

This work was performed through a project for the National Research Laboratory, supported by the Korea Institute of Science and Technology Evaluation and Planning.

REFERENCES

1. F.H. Nicoll, *Appl. Phys. Lett.* 9, 13 (1966).
2. S.W. Koch, H. Haug, G. Schmieder, W. Bohnert, and C. Klingshirn, *Phys. Status Solidi B* 89, 431 (1978).
3. F. Hamdani et al., *Appl. Phys. Lett.* 70, 467 (1997).
4. Z.K. Tang, G.K.L. Wong, and P. Yu, *Appl. Phys. Lett.* 72, 3270 (1998).
5. D.M. Bagnall, Y.F. Chen, Z. Zhu, and T. Yao, *Appl. Phys. Lett.* 73, 1038 (1998).
6. T. Akane, K. Sugioka, and K. Midorikawa, *J. Vac. Sci. Technol. B* 18, 1406 (2000).
7. H.K. Kim, S.-H. Han, W.-K. Choi, and T.Y. Seong, *Appl. Phys. Lett.* 77, 1647 (2000).
8. I. Barin, F. Sauert, E.S. Rhonhof, and W.S. Sheng, *Thermochemical Data of Pure Substances* (New York: VCH, 1989).
9. A. Poppl and G. Volkel, *Phys. Status Solidi (a)* 125, 571 (1991).
10. G.D. Mahan, *J. Appl. Phys.* 54, 3825 (1983).
11. S. Ruvimov, Z. Kiliental-Weber, J. Washburn, K.J. Duxstad, E.E. Haller, Z.-F. Fan, S.N. Mohammad, W. Kim, A.E. Botchkarev, and H. Morkoc, *Appl. Phys. Lett.* 69, 1556 (1996).
12. J.F. Moulder, W.F. Stickle, P.E. Sobol, and K.D. Bomben, *Handbook of X-ray Photoelectron Spectroscopy* (Eden Prairie, MN: Perkin-Elmer Corp., 1992).